Journal of Materials Chemistry A

Accepted Manuscript

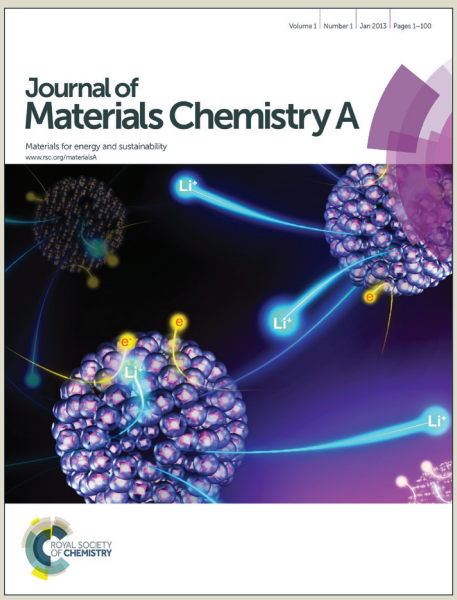

ROYAL SOCIETY OF CHEMISTRY

www.rsc.org/materialsA

Journal of Materials Chemistry A

Dynamic Article Links ►

Cite this: DOI: 10.1039/c0xx00000x

ARTICLE TYPE

www.rsc.org/xxxxxx

A simple route to transform normal hydrophilic cloth into Superhydrophobic-superhydrophilic hybrid surface

Ben Wang,[a,b] Yabin Zhang,[a,b] Weixin Liang,[a,b] Guiyuan Wang,[a,b] Zhiguang Guo*[a,b] and Weimin Liu[b]

Received (in XXX, XXX) Xth XXXXXXXXX 20XX, Accepted Xth XXXXXXXXX 20XX

DOI: 10.1039/b000000x

Metal nanoparticles are known as extremely hydrophilic substances due to their high surface energy. Hydrophobic property on the metal nanoparticles can be realized only if the nanoparticles were pretreated with low-surface-energy chemicals. In this paper, two adjacent transition metals, i.e. Fe and Co, were selected and coated on a commercial available fabric via a facile chemical in situ growth method. Then, *n*-octadecyl thiol, which possesses a low surface energy, was selected as the modifier to obtain superhydrophobic-superhydrophilic hybrid fabric depending on thiol's selective modification to Fe and Co nanoparticles on fabric. The surface Co nanoparticles can be modified by *n*-octadecyl thiol and transform into hydrophobic nanoparticles. However, the surface Fe nanoparticles cannot be modified *n*-octadecyl thiol in our experimental condition and thus still retain the hydrophilic property. An as-prepared fabric with these two kinds of nanoparticles even distributed on the surface is termed as superhydrophobic-superhydrophilic hybrid fabric since the fabric shows integral superhydrophobic property however possesses many superhydrophilic spots on the fabric. This material is hopeful to realize water harvesting like desert beetle collect water micro-droplet from the morning fog without exhausting external energy.

Introduction

In nature, various species have developed elegant schemes to adjust to their surroundings and win survival. Lotus leaves repel water and fouling very much so that they can ingeniously show themselves from sludge.[1] Water striders stand and skate upon a water freely due to the oriented patterned microsetae with fine nanogrooves on their legs.[2] Galapagos sharks move nimbly and quickly despite its awkward body because the close-packed dermal denticles (aligned parallel to the local flow direction of the water) all over their skin that can help reducing water drags.[3] Cactaceae species are known for their extremely drought-tolerant property which is ascribed to the special structure with well-distributed clusters of conical spines and trichomes on the cactus stem.[4] Desert beetles that reside in the areas of limited water collect water droplets from morning fog via their back which is covered with an alternating pattern of hydrophobic and hydrophilic microstructures.[5-7] The understanding of these functions offered by plants and animals gifted in nature can efficiently guide us to mimic and yield functional materials and devices.[8-10]

Learning from natural biological surfaces, various bio-inspired materials were reported aiming at gifting the surfaces with multifunctional properties (such as water-repellent, self-cleaning, and drag reduction property) and thus applying them to the fields of anti-fouling window glasses[11,12], micro-channels[13], oil/water separation[14,15] and water harvesting[16,25]. We have reported the multifunctional superhydrophobic surfaces such as transparent superhydrophobic glasses[17] and oil/water separation materials[15,18-22]. As the pure superhydrophobic surfaces were broadly investigated in the past decades[23-25], hybrid surfaces composed with both hydrophobic and hydrophilic ingredients have recently been studied and achieved by ornamenting hydrophilic spots on the superhydrophobic surface[16,26]. The hybrid surfaces show opposite wettability to the major water droplets and the minor water droplets. This kind of material is hopeful applying in the field of water harvesting and thus solving the global shortage of fresh water, especially for the remote areas with limited water (e.g. South Africa, North-west of China). Zhai et al. reported a patterned superhydrophobic-superoleophilic hybrid surface came from selective deposition of superhydrophobic multilayer films onto a hydrophilic patterns[16]. Ishii et al. prepared the biomimetic hybrid surface by electroless plating of self-organized honeycomb-patterned polymer films composed of metal-dome and polymer-spike superhydrophobic surfaces[26]. Chen et al. synthesized the perfectly hydrophobic nanfibers and selectively deposited polyelectrolytes onto the as-prepared hydrophobic surface[27]. Thickett et al. applied a spin-coating method to fabricate polymer bilayers with a hydrophilic polymer layer (equilibrium water contact angle (CA) 36.0°) on top of a hydrophobic polymer underlayer (equilibrium CA 91.3°) for atmospheric water capture[28]. However, these approaches often

either involve complicated synthetic procedures to introduce functional groups to the patterned areas or are limited by tedious manipulation to fabricate the hybrid surface, and the as-prepared hydrophobic-hydrophilic hybrid surface shows a small difference in the intrinsic wettability between hydrophobic spots and hydrophilic spots. Herein, an efficient in situ growth process was used to create superhydrophobic-superhydrophilic hybrid (SSH) fabrics, providing a simple and environment friendly method to acquire water harvesting property which previously required more complicated synthesis routes. The transition metal nanoparticles (NPs), Fe and Co, are served as the superhydrophilic ingredient and the superhydrophobic ingredient on fabrics, respectively. The two kinds of metal nanoparticles, under our controlled condition, can be selectively modified by low-surface-energy thiol (Co nanoparticles were modified whereas Fe nanoparticles were not). The modified Co nanoparticles show hydrophobic property whereas the unmodified Fe nanoparticles show hydrophilic property. To the best of our knowledge, such a selective modification strategy to fabricate superhydrophobic-superhydrophilic hybrid fabric has not been reported before. The coating amount of the NPs can be random controlled artificially and separately in a wide range via altering the concentrations and proportion of Fe(II) and Co(II) ions in the precursor solution. Meanwhile, the size of the SSH fabric required can be obtained in arbitrary scales via expanding the reaction apparatuses and thus make people convenient acquiring appropriate catchments capacity of the water within an optimal area of SSH. It is made from the costless fabric that can be randomly chosen from various textiles.

Materials and methods

Materials

The fabrics (containing 65% polyester and 35% cotton) were purchased from a local store in Lanzhou, China. The original fabrics were sequentially cleaned by distilled water, anhydrous ethanol and distilled water in an ultrasonic cleaner to remove possible impurities. *n*-Octadecyl thiol (96%) was obtained from Acros organics. All other chemicals were analytical-grade reagents and used as received.

Preparation of superhydrophobic-superhydrophilic hybrid fabrics

The as-cleaned fabric was immersed into a mixture of $Co(NO_3)_2$ and $FeSO_4$ solutions (3:1, totally 0.04 M) that provided the Fe and Co sources at room temperature under normal atmospheric conditions for 1-3 min. Next, an aqueous solution of sodium borohydride solution (0.03 M, 50 mL) was added dropwise into the precursor solution at room temperature under constant magnetic stirring. 30 min later, the fabric with Fe and Co nanoparticles grown on it was drawn from the solution and sequentially washed with distilled water and ethanol at least three times to eliminate the residual solution. The fabric then was dried in a drying oven for 10 min and immersed in 50 mL of 4 mM *n*-octadecyl thiol anhydrous ethanol for 24 h at room temperature. Finally, the fabric was thoroughly washed with copious amounts of anhydrous ethanol to remove any residual thiol and dried in a drying oven.

Characterization

The water contact angle was measured with a 5 μL distilled water droplet at ambient temperature with a DSA100 contact angle meter (Kruss Company, Germany). The average CA value was obtained by measuring the sample at five different positions, and the images were captured with a traditional digital camera. Scanning electron microscopy (SEM) images were obtained on JEOL JSM-5600LV and JEOL JSM-7100F scanning electron microscopes with Au-sputtered and Pt-sputtered specimens. X-ray energy dispersive spectrometer (EDS) attached to the scanning electron microscopes was used for the examination of the chemical composition of the as-prepared fabric. The amounts of Fe and Co nanoparticles present on the fabrics were determined by atomic absorption spectroscopy (AAS) (Analytik, Jena, contrAA700). The surface chemical composition and surface element content analysis of the as-prepared surfaces were investigated using X-ray photoelectron spectroscopy (XPS), which was conducted on a Thermo Scientific ESCALAB 250Xi electron spectrometer using the Al Kα line as the excitation source. The binding energy of C 1s (284.6 eV) was used as the reference. The air humidity was produced controlled by S20U-S ultrasonic humidifier (Midea, China).

Results and discussion

As-selected metal NPs (Fe and Co) can smoothly coated on the fabrics via an in situ growth process (Figure 1) because of the presence of different oxygen groups on fabrics that can easily bond with the metal NPs. The weights before and after the in situ growth process were measured and recorded to demonstrate that the NPs had been successfully coated on the fabrics (Table S1) and the increased weight is commonly about 2%~5% of the original fabric. After the thiol treatment, the Co NPs on the fabric were well modified whereas the Fe NPs on the fabric were unable to be modified with thiol. In order to demonstrate the inverse wettability of Fe and Co NPs after the thiol modification, we separately made the Fe NPs and Co NPs in situ growth on two vacant fabrics and followed by the thiol modification as schematically shown in Figure 2. The result clearly shows that the fabric coated with Co NPs showed superhydrophobicity whereas the fabric coated with Fe NPs still showed superhydrophilicity. It can be concluded that the Co NPs are readily to bond with thiol ligand whereas the Fe NPs on the fabrics are hardly coordinating with thiol-ligand without specialized treatment (such as prolonged drying in a drying oven and rinsed with sodium borohydride aqueous solution) as demonstrated by our previous reports.[15,18] The mechanism was illustrated as followed: The reduced single metal NPs on the fabric can be oxidized to the oxides more or less. Fe element generally exists by virtue of elemental Fe and Fe(III), Fe(II) in FeO and $Fe(OH)_2$ is quite oxidizable in the air so that it is hard to have the elementary Fe NPs to be oxidized to Fe(II). For Fe element, we can only find the pK_{sp} values of FeS (Fe(II)) from *Lange's Chemistry Handbook, 15th Edition* (pK_{sp}=17.20); both elemental Fe and Fe(III) are vacant. For Co element, the stable valence state is Co(II). As the outer surface of the Co NPs were oxidized to the Co(II), the Co(II) is readily coordinated with thiol (the pK_{sp} of CoS was 24.7). According to this difference between

Fe and Co, we successfully fabricated SSH fabrics from simultaneously in situ growth of Fe and Co NPs with thiol modification.

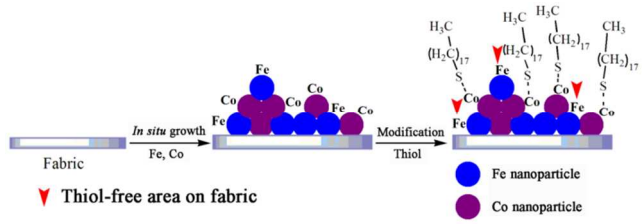

Fig. 1 Schematic illustration of the preparation procedure of the SSH fabric from in situ growth of Fe and Co NPs with thiol modification.

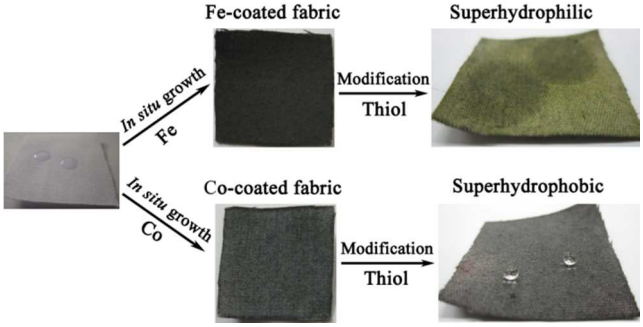

Fig. 2 The procedures of separately in situ growth of Fe and Co NPs. The final wettabilities were absolutely opposite.

Transition-metal NPs in the air quite likely form an oxidation layer at the outer surface. The oxidation layer is prone to coordinate with thiol and thus invert its wettability. Unfortunately, it is notable that the Fe is exceptive that cannot coordinated with thiol because the Fe(II) (willing to bond with thiol) is unstable in the air. The outer oxidation layer are mainly composed of Fe(III) that cannot interact with S ligand. The reason is that Fe(III) can oxidize S ions, Fe(III) would oxidize RSH to RS-SR and the RS-Fe(III) was thus not formed. Thus, the introduction of Fe NPs on the fabric is regarded as the superhydrophilic ingredient since the hydrophobic group (thiol ligand) cannot be smoothly fixed on the Fe NPs in the fabricating process. As for the other transition metal, Co, is a adjacent element of Fe in the periodic table of elements (Figure 3a). The redox potentials of them (φ(Co(II)/Co)=-0.277, φ(Fe(II)/Fe)=-0.44) are so closed that the in situ growth of Fe and Co occurred near-simultaneously, forming the homogenous hybrid surface. If the as-selected transition element possesses an oversize difference of the redox potential with φ(Fe(II)/Fe), the priority of the in situ growth process will dominate the fabricating procedure and lead the inhomogeneity of the in situ growth process layer by layer. As illustrated in Figure 3b-d, when we use the mixture composed with the equal concentrations of $Co(NO_3)_2$ (0.04 M) and $FeSO_4$ (0.04 M) as the precursor, the obtained fabric would have both of the two elements in situ growth on and peak intensities are approximate (Figure 3c and d). In contrast, as we use the mixture composed with the equal concentrations of $CuSO_4$ (0.04 M) and $FeSO_4$ (0.04 M) as the precursor which have a relatively larger redox potential between φ(Fe(II)/Fe) and φ(Cu(II)/Cu) (=0.340), the obtained fabric from the in situ growth method would mainly coated with Cu NPs. The peak intensity of Fe element in Figure 3g is quite weak compared to the peak intensity of Cu element in Figure 3f. Also, both the coating of Co and Fe NPs and Cu and Fe NPs were quantified by AAS analysis. The results showed a ratio of 0.82:1 for the coating of Co and Fe NPs and a ratio of 22.48:1 for the coating of Cu and Fe NPs, respectively. The results reflected that the competitive nucleation between Co and Fe NPs is fair whereas the competitive nucleation between Cu and Fe is violent. The metallic Fe can hardly be reduced before the metallic Cu have been completely reduced since the as-reduced Fe will immediately reduce the Cu(II) in the solution which possesses a higher redox potential (φ(Cu(II)/Cu)) even if the Fe(II) was supposed to be reduced. Here, as-selected Co element which is adjacent to Fe element can maximumly eliminate the inhomogeneity of the in situ growth process brought by the difference of the redox potentials as far as possible.

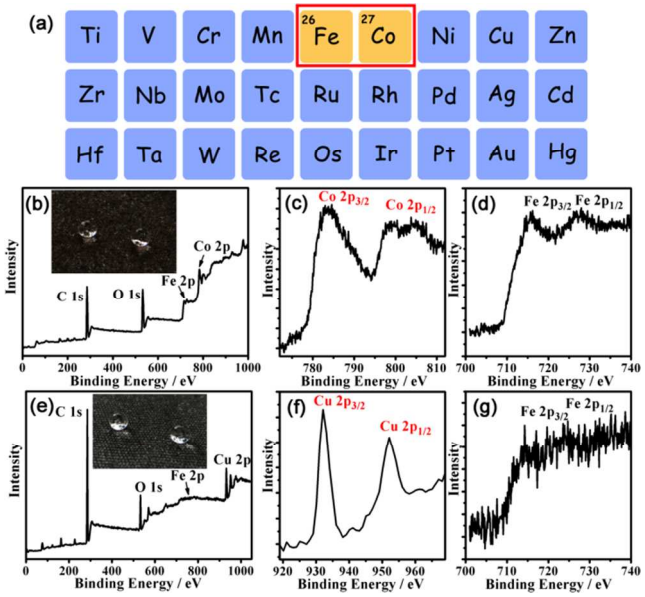

Fig. 3 (a) Graph showing a portion of periodic table of elements (b-d) XPS spectrum of as-prepared fabric from in situ growth of Co and Fe NPs with a equal concentrations Co(II) and Fe(II) ions in the precursor (c(Co(II))=c(Fe(II))=0.04 M). (e-g) XPS spectrum of the contrast experimental fabric from in situ growth of Cu and Fe NPs with a equal concentrations Cu(II) and Fe(II) ions in the precursor (c(Cu(II))=c(Fe(II))=0.04 M). Spectra in the far left column are integral spectra of the fabrics. The others are the high-resolution spectra corresponding to specific elements as labeled in the spectra. The insets in the left corner of (b) and (e) are the optical images of the as-prepared superhydrophobic fabrics.

The coating amount of Fe and Co NPs on fabric can be flexibly controlled via adjustment of the corresponding precursors. The former paragraph has depicted that the in situ growth of Fe and Co NPs did not have obvious priority from each other compared to the others since they have a less difference in the redox potentials. The random growth of the Fe NPs (hydrophilic ingredient), Co NPs (hydrophobic ingredient) and Fe-Co composite NPs on the fabric can be hardly recognized intuitively but demonstrated experimentally using the component analysis (AAS in Figure 4a, EDS and XPS in Figure S1). Meanwhile, we can artificially alter the amounts of Fe and Co NPs, as well as the size of the NPs via adjusting the concentration of precursors. Thus, precursors composed of Fe(II) and Co(II) ions with different concentration ratios were investigated in the

premise of maintaining the total concentration constant (0.04 M), aiming at revealing the wettability variance and guiding the designs the water harvesting fabric. The proportions of Fe and Co NPs coated on the fabric with different concentration ratios (c(Co(II))/c(Fe(II))) were determined by AAS (Figure 4a and Table S2 in the SI) and it was found that the proportions of as-reduced Fe and Co NPs n(Co)/n(Fe) on fabrics showed linear growth with respect to the ratio of c(Co(II))/c(Fe(II)) in the precursors. The coating ratio of n(Co)/n(Fe) on the fabrics shows nearly equal value to the ratio of c(Co(II))/c(Fe(II)). Meanwhile, the hydrophobic property gradually increases from the totally superhydrophilic to superhydrophobic with the increase of the ratio of c(Co(II))/c(Fe(II)) in the precursor. As shown by the optical images below the curve in Figure 4a, the wettabilities of the water droplet corresponding to different concentration ratio of Co(II) and Fe(II) (total concentration remains constant (c(Co(II))+c(Fe(II))=0.04 M)) are presented, which possess an increasing trend of contact angle as the increase of the concentration ratio c(Co(II))/c(Fe(II)). When the concentration ratio is quite low, which can induce a low coating capability of Co and a high coating capacity of Fe, the fabric is initially slightly hydrophobic but unstable (water spreads on the film and permeates through the film within about 96 s at the concentration ratio 1:4 and about 320 s at the concentration ratio 1:3), indicating that superfluous superhydrophilic ingredient and insufficient superhydrophobic ingredient are on fabric. As the concentration ratio increases to 1(coating ratio is about 0.86), the stable superhydrophobic fabric is obtained after the modification of n-octadecyl thiol. As the concentration continues to increase, the contact angle of water droplet on fabric will be slightly changed and remains at >150°. The surface morphologies of the SSH fabrics with the gradual increases of the concentration ratio were illustrated by the SEM images in Figure 4b and c, Figure 4d and e, Figure 4f and g, which correspond to the dot 2, 3 and 4 of the curve in turns (SEM images of original fabric, dot 1 and 5 are showed in Figure S2). Moreover, the geometric morphology variation from the Fe(II) ion dominant precursor to the Co(II) ion dominant precursor was specially illustrated in Figure S3. While the Fe(II) ion is dominant in precursor, the NPs coated on the fabric are mainly made of micro-scale flower-liked sphere with many nano-sheet in it. While the Co(II) ion is dominant, the NPs coated on the fabric are mainly made of micro-scale sheet. The amounts of the two kinds of structures are fair when we control the concentration ratio of the precursor equal to 1. It is believable that the difference between these surface morphologies is related with the respective nucleation property of the selected metals (Fe and Co). However, the surface morphologies of these as-prepared fabrics are not responsible for final hydrophobic or hydrophilic properties but served as a magnified factor to the wettability. Since the unmodified metal nanoparticles are generally superhydrophilic due to their native high surface free energy, the surface wettabilities of the fabric coated with metal nanoparticles are thus integral superhydrophilic before thiol modification. Only if the resultant fabrics are covered with sufficient amount of Co nanoparticles, the hydrophobic property of the resultant fabric can be realized after thiol modification. Therefore, the morphology, as well as the superhydrophobic and superhydrophilic properties can be artificially altered via changing the concentration ratio in the precursor. The increase of Co(II) is favor of the superhydrophobic property whereas the increase of Fe(II) is favorable for the superhydrophilic property. Unfortunately, oversized concentration ratio of Co(II) and Fe(II) ions is harmful to the application of water harvesting resulting in a poor efficiency of collecting water droplets, which will be theoretically analyzed in the latter theoretical section. Moreover, the relationship between the coating ratios of Fe and Co NPs and the ratio of Fe(II) and Co(II) in the precursor was also investigated by EDS and XPS measurements, as the assistant evidence shown in Figure S1 that show good agreement with the AAS measurement. The EDS spectrums of as-prepared hybrid fabrics with thiol modification are sequentially showed in Figure S4 and the intensity of the peak values can successively and intuitively reflect the amount of the corresponding NPs. As the integral (AAS) and partial (EDS and XPS) component analysis have the approximately accordant trend, it can be concluded that distributions of Fe and Co NPs are uniformly coated, forming the homogenous SSH fabrics.

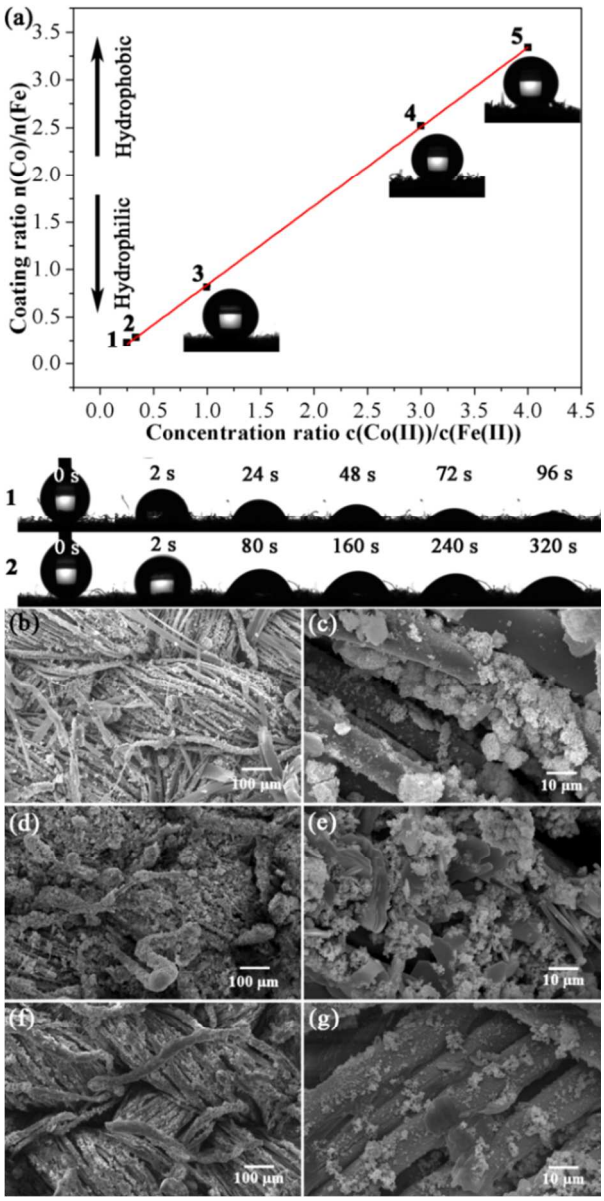

Fig. 4 (a) Relationship between the coating amount ratio of Co and Fe NPs (detected by AAS) and the concentration ratio of Co(II) and Fe(II) ions in the precursor. The optical images of contact angle at different concentration ratios after modification with n-octadecyl thiol are presented beside the curve (5 μL). The contact behaviors of water droplet at lower concentrations were proposed underneath. Panels (b-g) are SEM images corresponding to different concentration ratios of Co(II) and Fe(II) ions in the precursors as labeled with dots 1-5 in panel (a): (b, c) dot 2 (concentration ratio 1:3), (d, e) dot 3 (concentration ratio 1:1), (f, g) dot 4 (concentration ratio 3:1). SEM images in the left column are large-area view of the hybrid fabrics whereas images in the right column are high-resolution SEM images.

Inspired by the desert beetles that can adhere, handle and collect water microdroplets without using an external energy source, the SSH fabrics was fabricated aiming at collecting freshwater from the morning fog. The superhydrophilic ingredients (Fe NPs) on the as-prepared fabric can adhere and fix the microdroplets, the microdroplets will gradually grow up and eventually stop spread outward as the water droplet arrived at the boundary of the superhydrophilic ingredient and the superhydrophobic ingredient. Then the microdroplets will be pinned on the superhydrophilic spot and finally get rid of the superhydrophilic spot (rolling off) due to the integral superhydrophobicity of the fabric. It is inferred that the SSH fabric will began to harvest water droplet while the pinning velocity of water droplet is larger than the evaporating velocity. The water harvesting process is essentially the competition between condensation and evaporation and thus can be realized in a sufficient humid environment. Here, the water harvesting test was proposed by using the ultrasonic humidifier (Figure S5) to produce water mist environment in a 50×30×30 cm^3 sealed box (Temperature was 19 ± 1 °C and humidity was 72%). The pinning and condensation process of fogs on the SSH fabric with a concentration ratio of 3:1 was captured by a digital camera with discrete times ranging from 3 min to 90 min as shown in Figure 5. To the theory suggested by Chen et al.[29], three stages exist on a superhydrophobic surface without any external forces, namely *initial growth without coalescence*, *immobile coalescence* and *mobile coalescence*. At first the water drops on fabric nucleated and grew without significant interactions and the initial coverage of droplets can be negligible (Figure 5a and b). Then, the surface coverage of droplets is large enough and thus the droplets merged with the neighbor droplets frequently without external forces but remaining the center of mass of the merging droplets unchanged as schematically shown in Figure 5c and d. Finally, the self-propelled coalescence will lead to the mobilization and removal of the as-merged droplets from fabric as the average droplet diameter arrives at a threshold value (Figure 5e and g). The average diameter of droplets (d) on the fabric gradually increases with the time (t) and the relationship can be expressed as[30]

$$\langle d \rangle \sim t^{\alpha}$$

where α is the growth law exponent depending on the stage of condensation. As the time consumed, droplets will reach the threshold diameter and get rid of the surface. Henceforth, the water initial growth, coalescence and condensation will reach a dynamic equilibrium and the integral weight of the fabric will remain unaltered which is considered as the last and main stage for the water harvesting process. Another test was proposed to quantitatively study the water harvesting ability of the fabrics and optimize the concentration ratio.

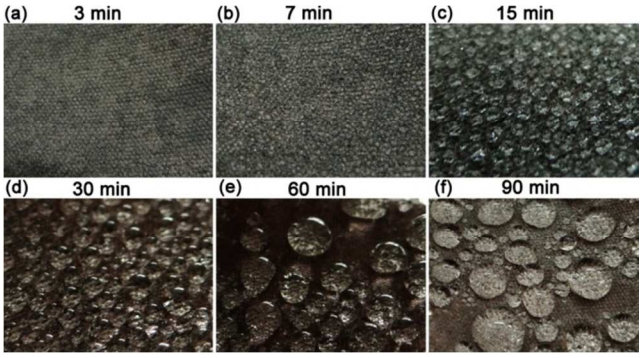

Fig. 5 Optical images of harvested droplets with different times (a) 3 min (b) 7 min, (c) 15 min, (d) 30 min, (e) 60 min and (f) 90 min.

As the water harvesting property was commonly suggested for a integral superhydrophobic surface, we applied the as-prepared superhydrophobic fabrics (Upper surface area=3×3 cm^2) with concentration ratio of 1:1 and 3:1 to collected water in a 50×30×30 cm^3 semi-sealed box. In the whole water harvesting process, the environmental temperature was maintained at 19 ± 1 °C and the resultant SSH fabrics were exposed to 72% humidity. As schematically shown in Figure 6, the net weight of water collected by as-prepared fabric was an increasing function of time. The net weight of water is approximate to zero during the initial period of time, indicating the stage of *initial growth without coalescence*. However, the net weight of water will get an increase while the time surpasses one certain value and then increase steadily with time, indicating the advent of *mobile coalescence*. It is considered that the superhydrophilic ingredients play an important role in a water harvesting process. Surprisingly, as for the variation trend showed in Figure 6, it can be observed that the net weight of water collected by as-prepared fabrics with difference amounts of superhydrophilic ingredients show actually little difference while it meets its steady increase stage (about 120 min later). This might because that the superhydrophilic ingredients play little role while they were wholly covered by the growing droplets. The later absorption of water fog is completely dependent on the growing droplets on fabrics since only the outer surface of the as-condensed droplet can get in touched with the fogs in air (Figure 5d). The superhydrophilic ingredients on the fabric cannot contact the external fogs due to the block effect of the as-condensed droplet on the fabric. While the droplet on the fabric expanded to an ample size, the droplet will sliding off the surface and the bared superhydrophilic nanoparticles can resume the second generation of water harvesting procedure. From the first half of the curve, it was observed that the superhydrophilic ingredient can affect the initial starting time of the collection of as-prepared fabric. The SSH fabric with a concentration ratio of 3:1 started to harvest water at 60 min whereas as the SSH fabric with a concentration ratio of 1:1 started to harvest water at 90 min (Figure 6). The fabric with a concentration ratio of 3:1 shows an earlier time to collect the first drop of water than that of the fabric with a concentration ratio of 1:1 that was reflected by the starting time of the water net weight increasement. The well sliding ability of the SSH fabric with the higher concentration ratio makes the collection of water easy-proceeding at a lower sliding angle. Contrarily, the increase of the amount of hydrophilic ingredients on fabric will delay the initial starting time of the water collection. As the amount of superhydrophilic ingredients

is not conclusive for the water harvesting process and the overmuch superhydrophilic ingredient will contrarily hamper the collection of water due to the competition behavior between hydrophobic ingredients and hydrophilic ingredients, the fabrics with a bigger concentration ratio will be more proper. However, the water harvesting cannot proceed without the hydrophilic ingredients. As for the as-prepared fabric with a concentration ratio of 3:1, the average collecting rate, i.e. the average net weight of water per unit area and per unit time, after the water harvesting reaches the steady increase stage is calculated of about 520 $g \cdot m^{-2} \cdot h^{-1}$. As the water consumption of the ultrasonic humidifier per hour is about 290 g, the water collection efficiency, i.e. the net water collected by the 3.0×3.0 cm^2 fabric per hour in a box of 50×30×30 cm^3 at 19 ± 1 °C divided by the total water consumed by the ultrasonic humidifier, is calculated of about 0.16%. The water collection efficiency is not satisfied. However this brand-new strategy for constructing superhydrophobic-superhydrophilic hybrid fabric is quite easily to be scaled up than the ever-reported methods.

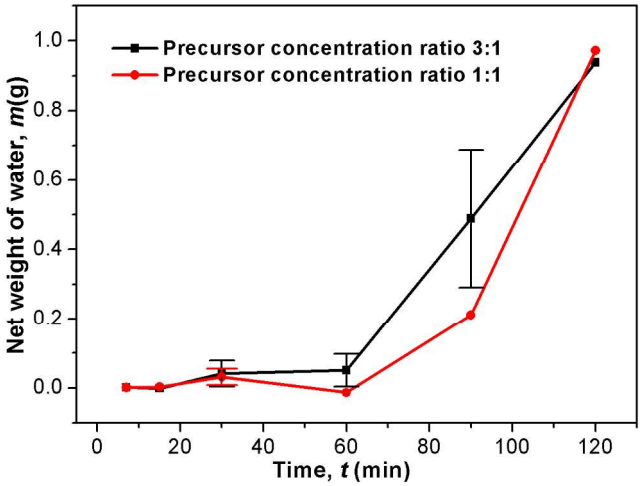

Fig. 6 Line graph showing the relationship between the net weight of water and the time at a concentration ratio of 3:1 and 1:1. The net weight of water shows an obviously increase while the time surpass 30 min.

The micro-scale morphology is obtained by SEM as showed in Figure 4f and g, and the composition was determined by EDS and XPS spectra as graphically shown in Figure 7. The EDS maps of Fe, Co and S elements are presented in Figure 7d. The Fe, Co and S elements are all uniformly distributed on the surface of fabric, which further demonstrated the superhydrophilic and superhydrophobic nanoparticles are randomly and evenly existed all over the fabric surface. In addition, the cycle experiment was proposed to study the recyclability of as-prepared fabric in the application of water harvesting. Specifically, the integral CA for a 5 μL droplet after every one-hour water harvesting test was used to evaluate the recyclability of as-prepared fabric at the precursor concentration ratio c(Co(II))/c(Fe(II))=3. As shown in Figure S6, the resultant SSH fabrics still exhibited good superhydrophobic property after 12 times repetitions, though the color of the SSH fabric got lighter than the unused one (Figure 7a). Moreover, the EDS spectrum and EDS maps of Fe, Co and S elements revealed that the SSH fabric still possessed even distribution of the superhydrophobic and superhydrophilic ingredients on the fabric surface after repeatedly use for water harvesting. In addition, the water contact angles of the as-prepared SSH fabric were recorded within the 12-times recycling as shown in Figure S7, which illustrated the good recyclability and reusability of the SSH fabric.

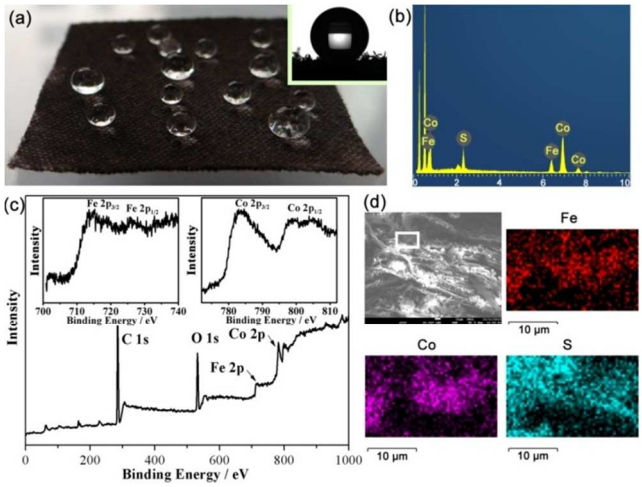

Fig. 7 (a) Optical images of macroscale water droplets on the as-prepared fabric with the precursor concentration ratio of 3:1. The inset shows the water CA of the fabric. (b) EDS spectrum of the resultant SSH fabric. (c) XPS spectra of the resultant SSH fabric. (d) The EDS maps of Fe, Co and S elements on the resultant SSH fabric.

The Fe NPs have good affinity for water and, therefore, affect the adhesion properties of water microdroplets on the hybrid surface. Since the roll-off of water droplet from the fabric implies its collection, the roll-off angle (α, $0 \le \alpha \le 90°$) can be investigated to elucidate the water harvesting ability. With the accumulation of the droplet, it will eventually slide down the inclined fabric. As for the second of the droplet's sliding, the adhesion force of the fabric exerted to the droplet can be calculated as[31]

$$F = mg\sin\alpha = 1/6\pi D^3 \rho g \sin\alpha \quad (1)$$

where F is the adhesive force, m represents the mass of the water droplet, ρ represents the density of water and D represents the diameter of the water droplet. In addition, for the surface micro-structure, the adhesive force can be also expressed as[31]

$$F = NSF_0 \quad (2)$$

where N represents the areal number density of the superhydrophilic Fe NPs. S represents the apparent contact area with the water droplet with a given mass m, and F_0 is the adhesive force of a single superhydrophilic Fe nanoparticle in the premise of supposing uniform and equal-sized NPs were formed on the fabric. By combining eqns (1) and (2), we obtained

$$\sin\alpha = 6NSF_0/(\pi D^3 \rho g) \quad (3)$$

$\sin\alpha$ is the monotonous increasing function of α in the range $0 \le \alpha \le 90°$. From this equation, we can see that the roll-off angle (α) is the increasing function of NS which represent the intrinsic property of fabric whereas the decreasing function of D which represents the physical property of water droplet (Figure S8). Generally, on the one hand, as the superhydrophilic ingredient on the fabric, Fe NPs can collect and fix the microdroplets in the morning fog that is crucial for the water harvesting; on the other hand, the increasing proportion of Fe NPs on the fabric will increase the adhesive force between water droplet and the fabric

and thus increase the roll-off angle of water droplets (Figure S8a). It is disadvantageous for the water harvesting. Therefore, the applicable fabrics must contain appropriate Fe NPs coated on them and macroscopically show superhydrophobic property. Moreover, the size of the water droplet itself can affect the water harvesting process (Figure S8b). The oversized droplets are favor of rolling off the fabric whereas the undersized droplets are so difficult to overcome the surface adhesive force unless they wait their expansion.

Conclusion

In conclusion, we have successfully fabricated the superhydrophobic-superhydrophilic hybrid fabrics by utilizing the selective modification of *n*-octadecyl thiol to the coated Fe and Co NPs on fabrics that can be used as a potential water harvesting material with very low-cost, pollution-free agents and facile approach. Fe and Co NPs coated on the fabrics are randomly distributed and the coating amount of them is easy-to-controlled just by altering the concentrations and the proportion of Fe(II) and Co(II) ions in the precursor solution. Due to the selective modification between thiol and the NPs, the wettability of the fabrics is linearly dependent of the concentration ratio of Co(II) and Fe(II) ions in the precursor and varies in a wide range from superhydrophilic (totally use the Fe(II) ions as the precursor) to superhydrophobic (concentration ratio about 1:1). In order to obtain a water harvesting fabric, the concentration ratio must be appropriate since neither too small (Fe nanoparticle is dominant) nor too large ratio values (Co nanoparticle is dominant) are unbeneficial for the water harvesting process. This kind of material might motivate people to solve the global shortage of fresh water via an energy-saving strategy. However, how to improve the efficiency of the water harvesting process and minimize the critical volume value for the water to roll-off is still a challenge that need for further researches.

Acknowledgments

This work is supported by the National Nature Science Foundation of China (NO 31070155, 11172301 and 21203217), the "Funds for Distinguished Young Scientists" of Hubei Province (2012FFA002), the "Western Light Talent Culture" Project, the Co-joint Project of Chinese Academy of Sciences and the "Top Hundred Talents" Program of Chinese Academy of Sciences and the National 973 Project (2013CB632300) for financial support. We acknowledge Dr Jiazheng Zhao for SEM and EDS measurements.

Notes and references

[a] *Ministry of Education Key Laboratory for the Green Preparation and Application of Functional Materials and Hubei Collaborative Innovation Centre for Advanced Organic Chemical Materials, Hubei University, Wuhan 430062, People's Republic of China. Fax: 0086-931-8277088; Tel: 0086-931-4968105; E-mail: zguo@licp.cas.cn*

[b] *State Key Laboratory of Solid Lubrication, Lanzhou Institute of Chemical Physics, Chinese Academy of Sciences, Lanzhou 730000, People's Republic of China*

† Electronic Supplementary Information (ESI) available: Weight variations of as-dried SSH fabrics before and after in situ growth (Table S1), relationship between the coating amount ratio of Co and Fe nanoparticles (detected by EDS and XPS, Fig. S1), contents of the as-coated Fe and Co nanoparticles on the fabrics measured by AAS (Table S2), SEM images of the original fabric and the as-prepared ones corresponding to different concentration ratios of Co(II) and Fe(II) ions (Fig. S2), SEM images of the original fabric and the as-prepared ones corresponding to different concentration ratios of Co(II) and Fe(II) ions (Fig. S3), EDS spectra of the as-fabricated SSH fabrics from in situ growth of Co and Fe nanoparticles with different precursor concentrations (Fig. S4), photograph of the ultrasonic humidifier (Fig. S5), Optical image, SEM image, EDS spectrum and maps of as-prepared fabric with the precursor's concentration ratio 3:1 (Fig. S6), recyclability (Fig. S7), Theoretical prediction of the relationship between the roll-off angle and the total area formed by the superhydrophilic Fe nanoparticles, the diameter of the water droplet (Fig. S8). See DOI: 10.1039/b000000x/

1 W. Barthlott and C. Neinhuis, *Planta*, 1997, **202**, 1-8.
2 X. F. Gao and L. Jiang, *Nature*, 2004, **432**, 36-36.
3 D. W. Bechert, M. Bruse and W. Hage, *Exp. Fluids*, 2000, **28**, 403-412.
4 J. Ju, H. Bai, Y. M. Zheng, T. Y. Zhao, R. C. Fang and L. Jiang, *Nat. Commun.*, 2012, **3**, 1247.
5 A. R. Parker and C. R. Lawrence, *Nature*, 2001, **414**, 33-34.
6 M. K. Seely and W. J. Hamilton, *Science*, 1976, **193**, 484-486.
7 M. K. Seely, *Oecologia.* 1979, **42**, 213-227.
8 Z. G. Guo, F. Zhou, J. C. Hao and W. M. Liu, *J. Am. Chem. Soc.*, 2005, **127**, 15670-15671.
9 Z. G. Guo and W. M. Liu, *Plant Science*, 2007, **172**, 1103-1112.
10 Z. G. Guo, W. M. Liu and B. L. Su, *J. Colloid Interface Sci.*, 2011, **353**, 335-355.
11 R. G. Karunakaran, C.-H. Lu, Z. H. Zhang and S. Yang, *Langmuir*, 2011, **27**, 4594-4602.
12 B. Bhushan and Y. C. Jung, *Prog. Mater. Sci.*, 2011, **56**, 1-108.
13 C.-H. Choi, U. Ulmanella, J. Kim, C.-M. Ho and C.-J. Kim, *Phys. Fluids*, 2006, **18**, 087105.
14 B. Wang and Z. G. Guo, *Chem. Commun.*, 2013, **49**, 9416-9418.
15 B. Wang, J. Li, G. Y. Wang, W. X. Liang, Y. B. Zhang, L. Shi, Z. G. Guo and W. M. Liu, *ACS Appl. Mater. Interfaces.*, 2013, **5**, 1827-1839.
16 L. Zhai, M. C. Berg, F. Ç. Cebeci, Y. Kim, J. M. Milwid, M. F. Rubner and R. E. Cohen, *Nano Lett.*, 2006, **6**, 1213-1217.
17 Y. Chen, Y. B. Zhang, L. Shi, J. Li, Y. Xin, T. T. Yang and Z. G. Guo, *Appl. Phys. Lett.*, 2012, **101**, 033701.
18 J. Li, L. Shi, Y. Chen, Y. B. Zhang, Z. G. Guo, B.-L. Su and W. M. Liu, *J. Mater. Chem.*, 2012, **22**, 9774-9781.
19 W. X. Liang and Z. G. Guo, *RSC Adv.*, 2013, **3**, 16469-16474.
20 B. Wang and Z. G. Guo, *Appl. Phys. Lett.*, 2013, **103**, 063704.
21 B. Wang, Z. G. Guo and W. M. Liu, *RSC Adv.*, 2014, DOI: 10.1039/C3RA48002J.
22 J. W. Zeng and Z. G. Guo, *Colloids and Surfaces A: Physicochem. Eng. Aspects*, 2014, **444**, 283-288.
23 H. Y. Erbil, A. L. Demirel, Y. Avci and O. Mert, *Science*, 2003, **299**, 1377-1380.
24 A. Tuteja, W. Choi, J. M. Mabry, G. H. McKinley and R. E. Cohen, *Proc. Natl. Acad. Sci. U.S.A.*, 2008, **105**, 18200-18205.
25 G. Azimi, R. Dhiman, H. M. Kwon, A. T. Paxson and K. K. Varanasi, *Nat. Mater.*, 2013, **12**, 315-320.
26 D. Ishii, H. Yabu and M. Shimomura, *Chem. Mater.*, 2009, **21**, 1799-1801.
27 R. G. Chen, X. G. Zhang, Z. H. Su, R. Gong, X. Ge, H. J. Zhang and C. Wang, *J. Phys. Chem. C.*, 2009, **113**, 8350-8356.
28 S. C. Thickett, C. N. Neto and A. T. Harris, *Adv. Mater.*, 2011, **23**, 3718-3722.
29 J. B. Boreyko and C. H. Chen, *Phys. Rev. Lett.*, 2009, **103**, 184501.
30 D. Beysens, *Atmos. Res.*, 1995, **39**, 215-237 .
31 D. Ishii and M. Shimonmura, *Chem. Mater.*, 2013, **25**, 509-513.

Abstract Graphic

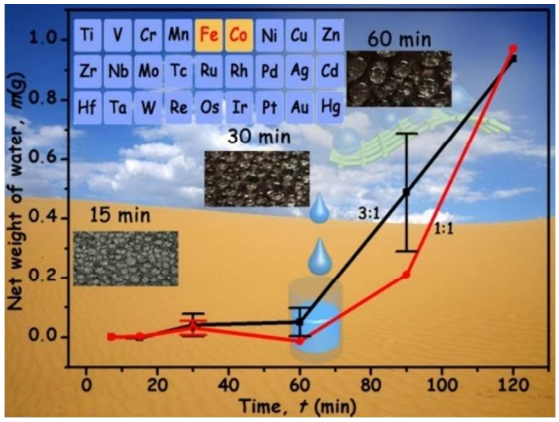

By utilizing the selective modification of *n*-octadecyl thiol to the Fe and Co nanoparticles, we fabricated superhydrophobic-superhydrophilic hybrid fabrics by simple in situ growth process.